APPLICATION OF TRANSITION MODELLING IN CFD FOR USE WITH TURBINE BLADES

Dwain Dunn[1]
Glen Snedden
Thomas Roos
CSIR
Pretoria, Gauteng,0001
South Africa
Email: [1]ddunn@csir.co.za

Thomas Hildebrandt

NUMECA Ingenieurbüro
Türkeistrasse 11
D-90518 Altdorf b. Nürnberg
Germany

Abstract

The design of internally-cooled gas turbine blades requires accurate predictions of distributions of blade temperature values and temperature gradients. This requires accurate predictions of heat transfer distributions from the hot gas (on the blade external surfaces) and the coolant (on the blade internal cooling passage surfaces). Navier-Stokes solvers assume the flow to be either fully laminar or fully turbulent, and solve accordingly.

The current validation test was designed to characterise the turbine blade external surface heat transfer predictive capability of a commercial RANS solver, which was augmented by a transition onset model, and compare the predictive accuracy with that of a boundary layer solver which also utilised a transition model. The validation case chosen was that of Consigny and Richards, in which blade Reynolds number, free stream turbulence degree, downstream Mach number and incidence angle were all varied independently.

Four turbulence modelling options have been tested as part of this study. In general it was found the following observations held true. Pressure surface heat transfer was acceptably well predicted by all turbulence models, including the boundary layer solver. On the suction surface accuracy of prediction was best achieved by the addition of the transition model (as in the boundary layer and Spalart-Allmaras with transition) compared to those without (Yang-shih k-ε and Spalart-Allmaras without transition).

The boundary layer solver consistently gave good results on the suction surface. The Spalart-Allmaras turbulence model with Abu-Ghannam and Shaw and intermittency model over predicted suction surface heat transfer least of the turbulence models by predicting the latest transition, however transition was still too early, as expected when using 2D geometry. The Yang-Shih k-ε turbulence model over-predicted the suction surface heat transfer, but no transition model was used. While the Spalart-Allmaras without transition over predicted the suction surface heat transfer by implying fully turbulent heat transfer, which was to be expected.

Nomenclature

b2b Blade-to-blade
C, c Chord
CFD Computational Fluid Dynamics
e Turbulent dissipation rate
γ_t Intermittency length
k Turbulent kinetic energy
l Length scale
ν Kinematic viscosity
n Spot formation rate
μ Viscosity
Ma Mach number
Re_ϑ Momentum thickness Reynolds number
SA Spalart-Allmaras
s Surface distance from stagnation point
s Spot propagation parameter
TET Turbine Entrance Temperature
T_u Turbulence degree
$\overline{U}$ Average free stream velocity
x Distance from blade leading edge
x_t Transition onset location
y^+ Near wall Reynolds Number

Subscripts:
1 Inlet
2 Outlet
∞ Freestream
is Isentropic
t Turbulent
T Total

Introduction

In an attempt to improve turbine efficiencies, turbine manufacturers are continually striving to increase the turbine entrance temperature (TET). However the TET values used presently are high enough to affect the structural integrity of blade materials. Thus cooling passages inside the blade are used to cool the blade, helping to prevent thermal damage. These cooling passages then bleed coolant air into the turbine through various film cooling locations to create a cool layer around the blade to prevent contact with the hot gas.

To maximise the effectiveness of the cooling flows however it is necessary to accurately predict the heat transfer. Navier-Stokes predictions of heat transfer are desirable. Unfortunately the use of Navier-Stokes solvers to predict heat transfer distributions to gas turbine blade surfaces has not been satisfactory where stability-induced transition occurs upstream of the throat, such as on the suction surface of a turbine blade or vane without film cooling rows due to the effect of free stream turbulence.

One of the main causes of this is the inability of turbulence models to accurately capture the flow field due to the complexities of transition, and the assumptions made in order to calculate turbulence.

The approach followed by engine companies in this case was to make use of boundary layer codes with empirical transition onset and transition length correlations. Some workers such as Boyle [1] have attempted to introduce empirical transition modelling into Navier-stokes solvers, but without significant uptake by the turbomachinery community. As recent as 2006 Sveningsson [2] has stated that there is an increased need for accurate prediction of transitional boundary layers.

Dunn [3] stated that most CFD codes are able to predict the midspan surface pressure data at midspan well, but are not as accurate at the blade hub and tip. It was also stated that the heat transfer distributions were not as well predicted. With 3D predictions requiring more work. Johnson [4], quoting Simoneau *et al.* [5] states that a 2D simulation gives good insight into 2D like flows such as those at midspan. It should be noted however that this is not the case for flows close to the hub and shroud due to 3D flows, such as secondary flow vortices.

Maaroofi *et al.* [6] performed a 2D numerical study of the VKI blade profile using an in-house code. The grid contained 32 000 cells and had $0 < y^+ < 5$. Comparisons were made using the Baldwin-Lomax model as well as three variants of the k-ε turbulence model, namely the Chien, Launder and Sharma, and the Biswas and Fukuyama, as well as the two k-ω models of Wilcox. To improve the heat transfer predictions the k-ε model had the Yap modification applied, and the k-ω had the Kato-Launder modification applied [6]. They found that all the turbulence models tested could not accurately predict the heat transfer; the modifications did improve the correlations due to improved leading edge flow prediction. However no transition model was applied and intermittency was not taken into account in their investigation.

The current investigation aims at investigating the empirical transition model presented by Abu-Ghannam and Shaw (AGS) as implemented in a RANS solver, FINE^{TM}/Turbo was used, the results of which were compared to the predictions of STAN5 [7], a boundary layer code with the AGS model incorporated as found in [8].

Numerical approach

The boundary layer results presented were obtained using STAN5 [7], the numerical approach used can be found in Roos [8]. Numeca's FINE^{TM}/Turbo v8.3-1 was used for the Navier-Stokes results. The different codes used the same boundary conditions, which varied per case as described below.

When transition is modeled in FINE^{TM}/Turbo the momentum thickness Reynolds number Re_ϑ is calculated. For values of Re_ϑ less than the critical value calculated, the boundary layer is assumed to be laminar, and turbulent for values higher than the critical calculated value. Re_ϑ is calculated using [8]:

$$Re_\vartheta = 163 + \exp(691\text{-}100T_u) \quad (1)$$

Where Re_ϑ is the momentum thickness Reynolds number and T_u is the turbulence degree, expressed as a decimal. When intermittency is modeled there is a gradual change from the transition onset location predicted by Equation (1) according to:

$$\gamma t = 1 - \exp\left(-\frac{n\sigma(x - x_t)^n}{\alpha}\right) \text{ for } x \geq x_t \quad (2)$$

In order to reduce computational expense, the blade-to-blade (b2b) feature in FINE^{TM}/Turbo was utilised. The b2b feature allows for the use of a 2D mesh, consisting of a single layer of cells and is ideal for 2D cascade cases, where the aim is to minimise 3D effects. A 2D mesh has the advantage that there are fewer cells due to the reduced number of layers, as well as no endwall effects. The boundary layer grid was generated as an O-grid that was 33 cells wide, having an expansion ratio of 1.24. Figure 1 shows the mesh used, showing the boundary layer expansion in the region of the leading and trailing edge. The domain consisted of over 40 000 cells, with a y^+ ranging from $y^+ = 0.1$ to $y^+ = 2.5$. Figure 2 shows the y^+ distribution for the blades for the lowest average value (Case C1) and the highest average value (Case C4).

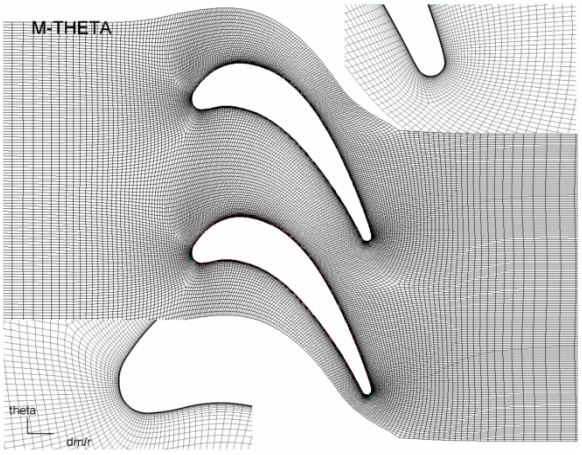

Figure 1: Navier-Stokes mesh used, showing leading edge and trailing edge cell clustering

Consigny and Richards [9] performed a large number of experiments that produced a large amount of data, and therefore not all of the test cases were presented here. The test cases to be presented are listed in Table 1, with only the lowest, $T_{u\infty} = 0.8$ % and the highest, $T_{u\infty} = 5.2$ % turbulent intensities presented. Even thought low free stream turbulence is not useful to a gas

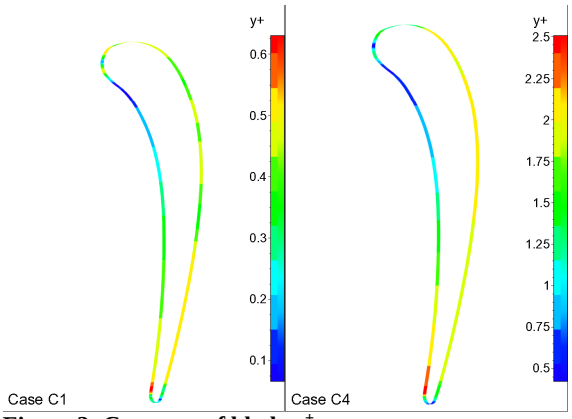

Figure 2: Contours of blade y^+

turbine designer [10], it was felt that if transition cannot be captured at low free stream turbulence levels it would be less likely that it will be captured at high turbulence levels.

Table 1: Experimental test conditions of the test cases to be investigated (reproduced from consigny and richards [9])

Test Case	Ma_1	Ma_{2is}	b_1	p_0 (bar)	T_0 (K)	T_w (K)	$(Re_c)1$ ($x10^{-5}$)
A	0.24	0.62	30°	1.275	419	296	3.385
B	0.278	1.15	30	2.07	419	294	6.315
C1	0.278	0.92	30	0.774	420	294	2.349
C4	0.278	0.92	30	3.071	417	294	9.421

The inlet was specified as having a uniform total pressure p_0, total temperature T_0, turbulent viscosity and flow vector (i.e. flow direction) for each of the relevant test cases in Table 1. The outlet boundary was a static pressure p_2 imposed outlet boundary. The blade surface was set as being isothermal at given wall temperature T_w. The working fluid was specified as air, using perfect gas correlations for gas properties.

FINE^{TM}/Turbo uses a density based approach for calculation of the transport equations. The current investigation was performed without using pre-conditioning, due to the high Mach Numbers.

For each test case, and each turbulent degree, five different cases were inspected, namely:

1. Euler boundary layer solver (STAN5) [7] with the transition model of Abu-Ghannam and Shaw [11] and the intermittency model of Dhawan and Narasimha [12] incorporated. The implementation was described in Roos [8].
2. Baseline: The low Reynolds number Yang-Shih k-ε turbulence model with varying inlet turbulence viscosity was chosen as the baseline for comparison, as it resolves the laminar sub-layer without resorting to a wall function approximation. For a detailed description of the turbulence model refer to [13].
3. Standard Spalart-Allmaras (SA) turbulence model with no transition modelling, so the flow is assumed to be turbulent everywhere. This can be used for low Reynolds Number flows as well. For a more detailed description of the turbulence model refer to [14]
4. Standard Spalart-Allmaras turbulence model with the transition model of Abu-Ghannam and Shaw [11], with stepwise intermittency model (eddy viscosity is fully turbulent after transition point). A detailed description of the transition model and the relevant equations can be found in [11]
5. Standard Spalart-Allmaras turbulence model with the transition model of Abu-Ghannam and Shaw [11] with the intermittency model of Dhawan and Narasimha [12], as incorporated in FINE^{TM}/Turbo via an expert parameter. For a detailed description of the intermittency model refer to [12]

The inlet turbulence viscosity for the Spalart-Allmaras turbulence model was calculated using the following equation [15, 16]:

$$\nu_t = \sqrt{\frac{3}{2}} \cdot \bar{u} \cdot T_u \cdot l \qquad (3)$$

where ν_t is the kinematic turbulent viscosity and l is the length scale. The length scale was taken as being l = 0.07C where C is the blade chord. For the Yang-Shih k-ε turbulence model k was calculated using [17]:

$$k = \frac{3}{2}\left(\sqrt{\bar{u}^2}\right)^2 \qquad (4)$$

and ε was calculated using

$$\varepsilon = u\frac{0.1k}{\Delta L} \qquad (5)$$

Where L is the characteristic length, in this case the blade chord was used. The domain was initialised with these values for all cases for the relevant turbulence models.

Results

A grid dependence study was performed to determine the appropriate size of the grid to be used. A factor of 4 was used to resize the grid (double mesh density in both directions in the plane perpendicular to the blade). The blade heat transfer and total pressure drop across the blade where compared for each grid size, as shown in Figure 3. As can be seen the results change very little between 40 000 and 180 000 cells, thus it was decided that 40 000 cells would be used since the grid met all the requirements of the turbulence models used [17], and a larger grid did not produce a significant difference in results.

Mach Number distribution

In Figure 4 to Figure 7 the Mach number predictions for cases A, B, C1 and C4 are compared for the different models. It can be seen that the stagnation point appears to

be poorly predicted by the Euler solver. This is because the Euler solver makes use of an H-grid, and the resolution is poor around the leading edge.

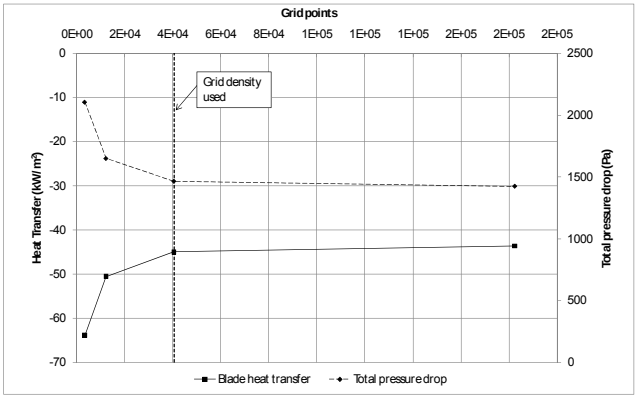

Figure 3: Blade heat transfer and total pressure drop with respect to grid density

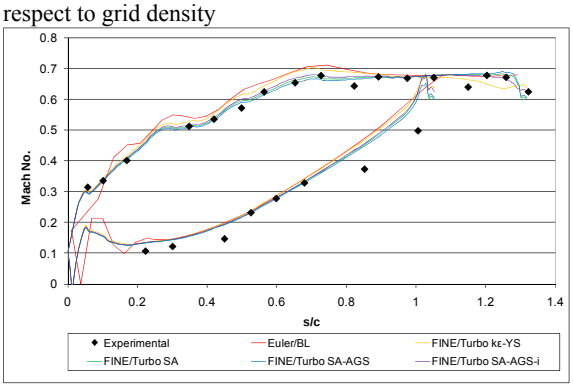

Figure 4: Case A: comparison of experimental and predicted Mach number distributions

Test case A, Figure 4 had a medium subsonic outlet velocity (Ma = 0.62), thus the flow can be seen to be subsonic everywhere, with the maximum velocity achieved on the suction surface in the throat. The Yang-Shih k-ε and Spalart-Allmaras turbulence models predict similar distributions of Mach number. All the predictions of the pressure surface Mach number agree with each other but not the experimental data. The reasons for the discrepancy given by Consigny and Richards (when they performed their boundary layer analysis in [9]) was that the static pressure tapping's near the trailing edge of the pressure surface, due to necessity made use of smaller diameter tubes than on the suction surface. Smaller diameter tubes

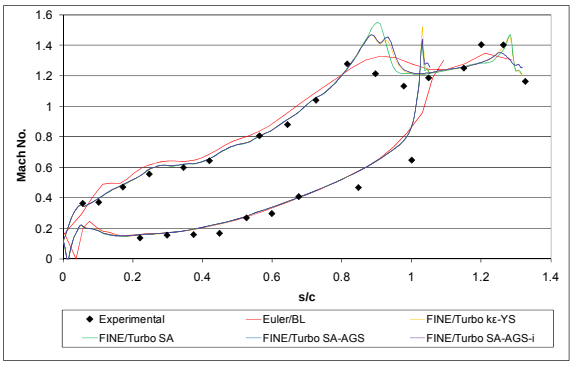

Figure 5: Case B: comparison of experimental and predicted Mach number distributions

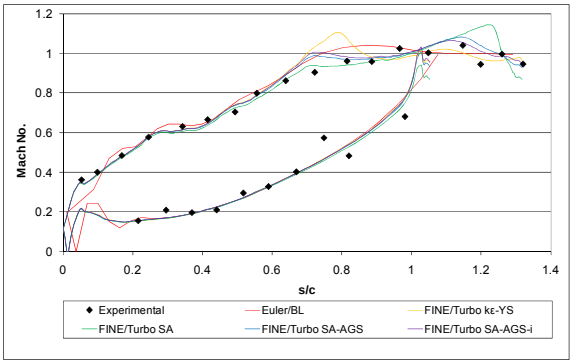

Figure 6: Case C1: comparison of experimental and predicted Mach number distributions

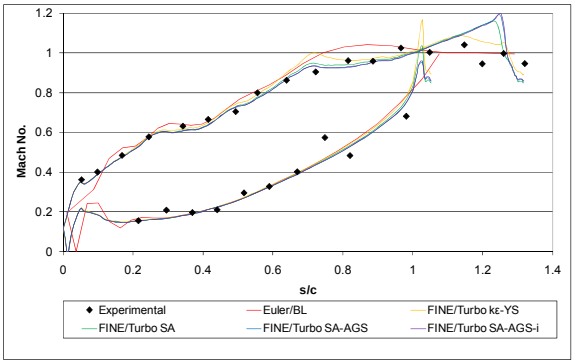

Figure 7: Case C4: comparison of experimental and predicted Mach number distributions

affect the response time and can lead to crimping and subsequent leaking. Test case B, Figure 5 had supersonic outlet velocity (Ma = 1.15). The wake flow was accelerated from the trailing edge by entrainment of the surrounding fluid until it was supersonic, allowing the suction surface expansion fan shocks to cut through the wakes and propagate out to the downstream boundary. The distributions of Mach number predicted by the Yang-Shih k-ε and Spalart-Allmaras turbulence models were again similar. Relative to the experimental data, all turbulence models appear to over-predict the shock strength, and predict the shock position late, of both the suction surface throat shock and the suction surface expansion fan shock. Here the Euler solver predictions were better than the RANS solver. The resolution of the pressure surface

experimental data was insufficient to conclude whether or not the pressure surface expansion fan shock was over-predicted.

In test cases C1, Figure 6 and C4, Figure 7, the Reynolds number was varied while the outlet flow was kept at Ma = 0.92. The Mach number distribution was well predicted compared with the experimental data, except at the suction surface expansion fan, where the Euler solver predictions were reasonable, but the Spalart-Allmaras variants tested perform better up to approximately s/c = 1.15. The Yang-Shih k-ε predicted a shock at the throat while the Spalart-Allmaras predicted a trailing edge shock for C1.

Heat transfer comparisons

Test case A

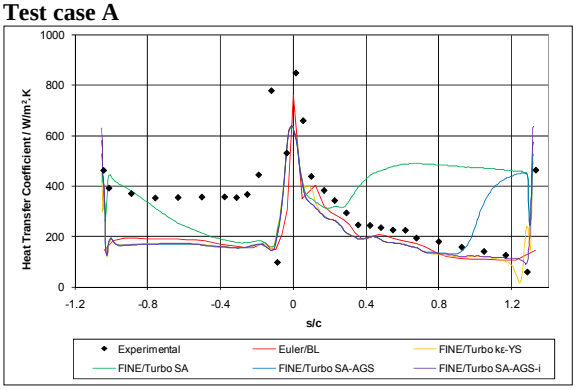

Figure 8: Case A: comparison of experimental and predicted heat transfer coefficient distributions for T_u = 0.8%

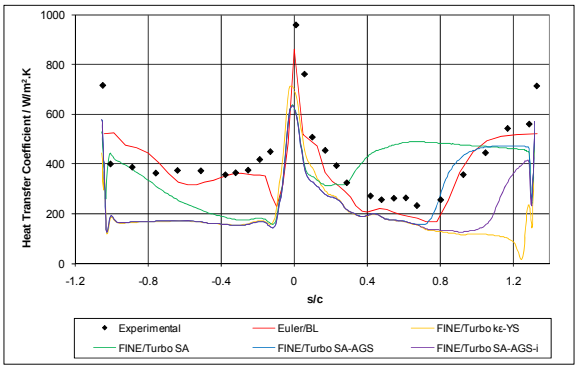

Figure 9: Case A: comparison of experimental and predicted heat transfer coefficient distributions for T_u = 5.2%

As mentioned previously, test case A was wholly subsonic. At T_u = 0.8%, Figure 8, a laminar separation bubble with downstream reattachment can be seen on the pressure surface just downstream of the leading edge. None of the models in either of the solvers were able to capture the high reattachment heat transfer at T_u = 0.8% (or the constant high heat transfer thereafter), although the boundary layer analysis indicates increased heat transfer due to reattachment for T_u = 5.2%, Figure 9. Unfortunately, pressure surface experimental data resolution was too poor at T_u = 5.2% to capture experimental separation and reattachment. Clues can be obtained, however, from test case C1, which at an inlet Reynolds number of Re = 2.349×10^5 was similar to that of test case A having an inlet Reynolds number of Re = 3.385×10^5. In test case C1 experimental evidence of pressure surface separation and reattachment can be seen.

The Yang-Shih k-ε model, in Figure 8 and Figure 9 predicted a pressure and suction surface heat transfer distribution indicative of completely laminar flow for both turbulence intensities. The Spalart-Allmaras model with no transition model, however predicted a heat transfer distribution indicative of transition at 25% chord irrespective of turbulence degree. The Spalart-Allmaras model with transition predicted a heat transfer distribution resembling transition at about 50% chord for T_u = 5.2%. The addition of the intermittency model improves the prediction of T_u = 0.8% turbulence case, however predicts late transition for the T_u = 5.2% case. The boundary layer code with transition performs very well, predicting the transition location and length for both turbulence levels.

Test case B

In test case B a shock occurred in the throat on the suction surface. The shock appeared to induce transition at T_u = 0.8% turbulence (Figure 10), while at higher turbulence intensity the transition point moves upstream, Figure 11.

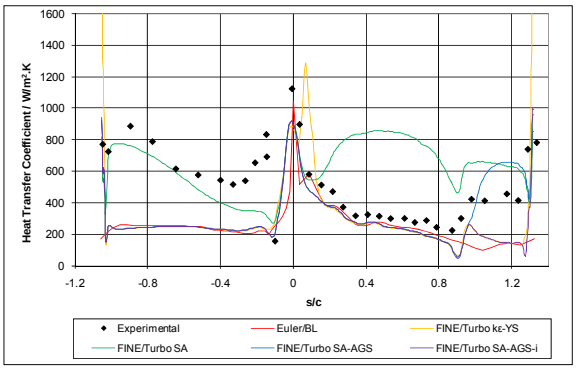

Figure 10: Case B: comparison of experimental and predicted heat transfer coefficient distributions for T_u = 0.8%

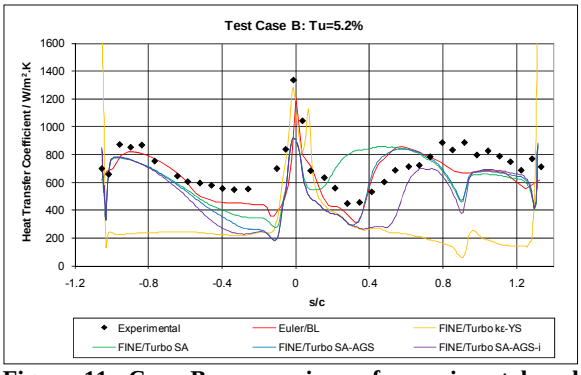

Figure 11: Case B: comparison of experimental and predicted heat transfer coefficient distributions for T_u = 5.2%

The laminar separation bubble can be seen in the T_u = 0.8% case, with high reattachment heat transfer not captured by the models.

Test case C1

The Yang-Shih k-ε model predicted a suction surface heat transfer distribution indicative of completely laminar flow (while predicting a second heat transfer peak on the suction surface just downstream of the leading edge for both turbulence degrees), while the Spalart-Allmaras model with no transition model predicts a heat transfer distribution indicative of transition at 10% chord irrespective of turbulence intensity. The Spalart-Allmaras with AGS transition model captures transition onset well for both turbulence intensities. The addition of improves

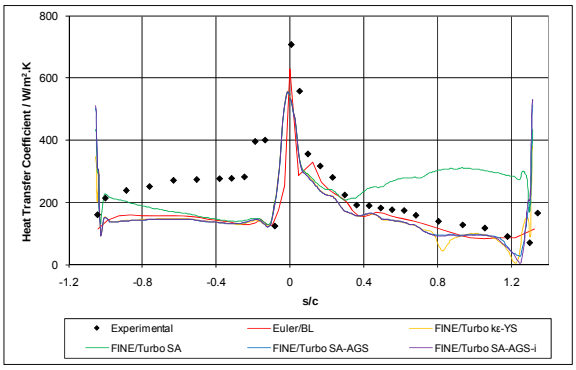

Figure 12: Case C1: comparison of experimental and predicted heat transfer coefficient distributions for T_u = 0.8%

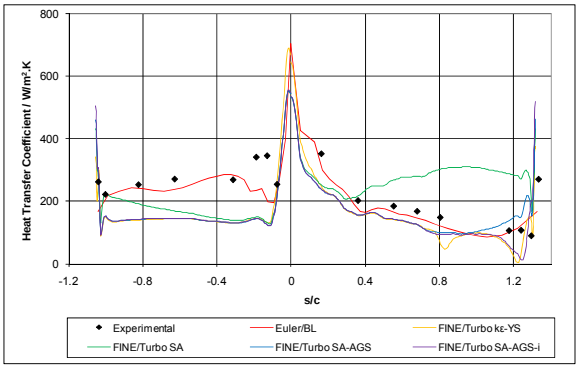

Figure 13: Case C1: comparison of experimental and predicted heat transfer coefficient distributions for T_u = 5.2%

the heat transfer prediction trend by increasing the implied transition length. The effect of the shock appears over predicted by the models. In test case C1, Figure 12 and Figure 13 (low Reynolds number, outlet Mach number of 0.92), the suction surface heat transfer is laminar for both turbulence intensities, and a separation bubble on the pressure surface reattaches and trips to turbulence. Most models predicted essentially laminar flow, except the boundary layer code at T_u = 5.2% that predicted the increased heat transfer downstream of the separation bubble. The SA model without transition predicted head transfer indicative of transition at 33% chord on the suction surface.

Test case C4

The C4 case is the highest Reynolds number of the four C cases. The Yang-shih k-ε model predicts a heat transfer distribution indicative of completely laminar flow, and a false heat transfer spike on the suction surface just downstream of the leading edge is seen for both T_u = 0.8% and T_u = 5.2% turbulence intensities Figure 14 and Figure 15. The SA without transition predicts a heat transfer distribution indicative of transition at less than 10% chord in each case. Spalart-Allmaras with transition model AGS predicts transition onset late for T_u = 0.8% and

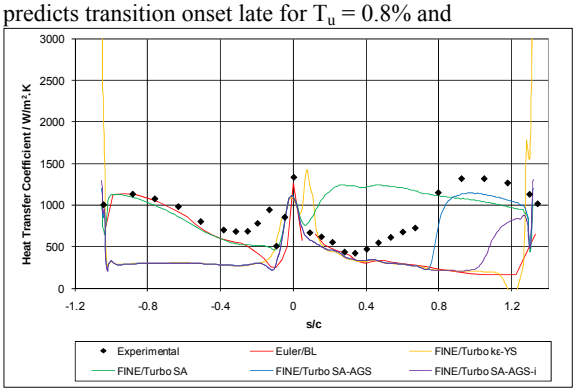

Figure 14: Case C4: comparison of experimental and predicted heat transfer coefficient distributions for T_u = 0.8%

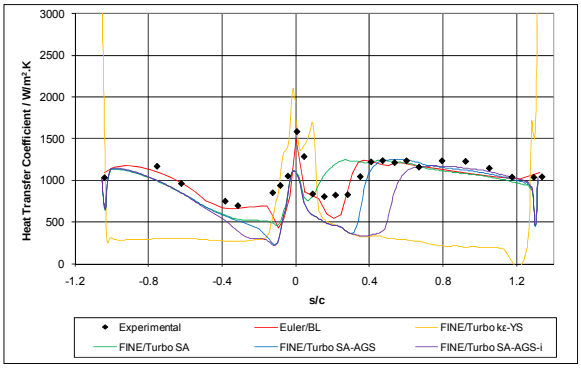

Figure 15: Case C4: comparison of experimental and predicted heat transfer coefficient distributions for T_u = 5.2%

approximately correctly T_u = 5.2%, while the addition of intermittency delayed effective transition to downstream of the experimental transition region. The boundary layer code, by comparison, incorrectly predicts essentially laminar flow for the T_u = 0.8% case, but like the SA with AGS, predicts transition in the T_u = 5.2% case accurately.

Conclusions

The Consigny and Richards [9] test case is rich and challenging, as so many variables are varied independently. This makes it an excellent test case for validation of numerical codes that predict heat transfer in the presence of transition.

The pressure surface heat transfer was predicted reasonably well by all turbulence models tested in FINE™/Turbo, as well as the boundary layer solver. The boundary layer solver however consistently gave good results on the suction surface. It should be noted that the boundary layer code does have limitations. It is purely 2D, does not handle unsteadiness and is not appropriate near endwalls where secondary flows can be expected.

The Spalart-Allmaras turbulence model with AGS and intermittency modelling under-predicted suction surface heat transfer by predicting transition later then the other models.

The Spalart-Allmaras turbulence model with AGS but without intermittency predicted suction surface heat transfer fairly accurately.

The Yang-Shih k-ε turbulence model over predicted suction surface heat transfer more than any other model by predicting essentially laminar flow on the suction surface

The Spalart-Allmaras turbulence model over predicted suction surface heat transfer worst by implying fully turbulent heat transfer.

From the above it can be seen that failing to introduce transition (as in the Yang-Shih k-ε and Spalart-Allmaras alone) does not effectively distinguish between laminar, transitional and turbulent regions, particularly on the suction surface. The addition of transition modelling is shown to greatly improve the heat transfer *distribution*, as can be seen in the predictions by the boundary layer solver and Spalart-Allmaras with AGS models. Unfortunately the addition of intermittency modelling as incorporated in the Spalart-Allmaras AGS implementation consistently predicts delayed transition, typically by 20% chord. Therefore given the limitations of boundary layer analysis, augmented by the generality implicit in a RANS analysis, the addition of transition modelling to a RANS solver (as implemented here in FINE™/Turbo) adds a powerful increase in heat transfer distribution prediction accuracy.

Aknowledgments

This document is the result of a research effort funded by the Defence Research Development Board under contract KT471006.

References

[1] Boyle, R., 1991. "Navier-stokes analysis of turbine blade heat transfer". Transactions of the ASME, Journal of Turbomachinery, 113, pp. 392–295.

[2] Sveningsson, A., 2006. Transition modelling – a review. Tech. rep., Division of Fluid Dynamics, Dept. of Applied Mechanics, Chalmers University of Technology, Gteborg.

[3] Dunn, M., 2001. "Convective heat transfer and aerodynamics in axial flow turbines". Journal of turbomachinery, 123(4), pp. 637–686.

[4] Johnson, J., 2006. Optimization of a low heat load turbine nozzle guide vane.

[5] Simoneau, R. J., and Simon, F. F., 1993. "Progress towards understanding and predicting heat transfer in the turbine gas path". International Journal of Heat and Fluid Flow, 14(2), pp. 106–128.

[6] Maaroofi, K., Nobari, M. R. H., and Shirani, E., 2007. "Progress towards understanding and predicting heat transfer in the turbine gas path". International Journal of Heat and Fluid Flow, 44(2), pp. 61–70.

[7] Crawford, M., and Kays, W., 1976. Stan5 a program for numerical computation of two-dimensional internal and external boundary layer flows: Cr-2742 stan5 manual. Tech. rep., NASA.

[8] Roos, T., 2009. "Validation of curvature correction models in the boundary layer code stan5". ISABE-2009-(1132).

[9] Consigny, H., and Richards, B., 1982. "Short duration measurements of heat transfer rate to a gas turbine rotor blade". Transaction of the ASME Journal of Engineering for Power, 104, pp. 542–551.

[10] Mayle, R. E., 1991. "The role of laminar-turbulent transition in gas turbine engines". Journal of Turbomachinery, 113, pp. 509–537.

[11] Abu-Ghannam, B., and Shaw, R., 1980. "Natural transition of boundary layers - the effects of turbulence, pressure gradient, and flow history". Journal Mechanical Engineering Science, 22(5), pp. 213–228.

[12] Dhawan, S., and Narasimha, R., 1958. "Some properties of the boundary layer flow during transition from laminar to turbulent motion". Journal of Fluid Mechanics, 3(5), pp. 418–436.

[13] Yang, Z., and Shih, T., 1993. "New time scale based k-epsilon model for near-wall turbulence". AIAA, 31(7), pp. 1191–1198.

[14] Spalart, P. R., and Allmaras, S. R., 1992. "A one-equation turbulence model for aerodynamic flows". AIAA, 92-0439.

[15] Ansys Fluent, 2007. Ansys Fluent manual. http://my.fit.edu/itresources/manuals/fluent6.3/help/html/ug/node217.htm#31661, February.

[16] CFD-Online, 2007. Turbulence free-stream boundary conditions. http://www.cfd-online.com/Wiki/Turbulence_free-stream_boundary_ conditions, February.

[17] Numeca, 2007. User Manual FINE/Turbo v8 (including Euranus) Documentation v8a, v8a ed. Numeca International, 5, Avenue Franklin Roosevelt, 1050 Brussels, Belgium, October.